NUMERICAL ANALYSIS OF THE DEVELOPING TIME IN TURBULENT DRAG REDUCING PLANE COUETTE FLOWS

Anselmo S. Pereira, anselmo.pereira@polytech-lille.fr[1]
Gilmar Mompean, gilmar.mompean@polytech-lille.fr[1]
Laurent Thais, laurent.thais@polytech-lille.fr[1]
Edson J. Soares, edson.soares@ufes.br[2]

[1]Université de Lille 1 - Sciences et Technologies, Polytech'Lille, and Laboratoire de Mécanique de Lille (LML), Cité Scientifique, 59655 Villeneuve d'Ascq, France.
[2]LabReo, Department of Mechanical Engineering, Universidade Federal do Espírito Santo, Avenida Fernando Ferrari, 514, Goiabeiras, 29075-910, ES, Brazil.

Abstract: *The addition of a small amount of polymers of high molecular weight can lead to a pressure drop decrease in turbulent flows. Over the years, numerous studies have been conducted in attempts to make practical use of polymer-induced drag reduction: long-distance transport of liquids, oil well operations, fire-fighting, transport of suspensions and slurries, and biomedical applications. However, many aspects concerning its main mechanism are yet unclear. One of those aspects is the initial development of the turbulent structures and polymer deformation over time. As an attempt to further understand the drag reduction over this developing time, we analyse a turbulent Couette flow of a FENE-P fluid by aiding of direct numerical simulation. We show that the initial interactions between the mean shear flow, turbulent structures, and polymer stretching are the key to understand the step-by-step evolution of the drag reduction (DR). Few instants after the beginning of the simulation, DR assumes expressive negative values before starting to increase and reaches its maximum value. When DR is minimum (in fact negative), polymers experience their highest deformation state. In other words, DR and polymer stretching evolve in an asynchronous way. A point which also deserves attention is the fact that the asymptotic value of the drag reduction is below its maximum one. We propose in this work to analyse the difference between the maximum drag reduction and its asymptotic value only by means of fluid dynamics.*
Keywords: *Drag reduction, Development time, Turbulent structures development, Direct numerical simulation, FENE-P model*

1. INTRODUCTION

Polymeric drag reducing flows has been analysed since the pioneering works of Forrest and Grierson (1931); Toms (1948); Mysels (1949). Among applications there is a great variety of process as fire-fighting operations, transport of liquids in pipes, transport overseas, blood flow resistance, and many others (Fabula, 1971; Burger and Chorn, 1980; Sellin *et al.*, 1982; Golda, 1986; Andrade *et al.*, 2016). The fundamentals of the drag reduction (DR) together with many of its practical aspects can be found in Lumley (1969, 1973); Virk (1975); Tabor and de Gennes (1986); White and Mungal (2008). From these papers one can mainly understand how concentration, molecular weight and temperature affect DR.

An aspect of DR that was not sufficiently analysed was its dependence on time, which is particularly expressive at the begging of the phenomenon and represents the main effort of this work. When polymers are introduced in a fully developed turbulent flow, they cause an abrupt disturbance. The mean shear flow and the turbulent structures are strongly changed and a new stead state takes time to be reached, as numerically shown by Dimitropoulos *et al.* (2005) and experimentally confirmed by Andrade *et al.* (2014). The drag reduction level can even assume negative values at the very beginning of the phenomenon (when polymers are injected in a turbulent flow, for example). In fact, DR is zero at the beginning and decreases until a minimum is reached, before starts to increase and achieve its maximum value after a significant period called the *developing time* (Pereira and Soares, 2012; Pereira *et al.*, 2013).

Despite the fact that DR has been widely studied, its transient aspect was not yet systematically carried out. Many doubts remain, as how it is the mutual relationship between polymers stretching and turbulent structures over time. We see here that such a relation is not obvious and sometimes, at least at a first glance, counter-intuitive. The focus of our work is to carefully analyse, by aiding of a numerical simulation of a FENE-P fluid, the transient aspects of drag reducing plane Couette flows during the developing time. The dependency of the turbulent structures and polymeric deformation on time is very complex and fundamental to fully understand the variations on the drag reduction level, which can even assumes negative values at the beginning of the simulations. In fact, the drag reduction is a consequence of the polymer deformation and its interaction with the turbulent structures. The evolution of DR over time is confronted here with the evolution of polymer stretching and turbulent structures. In addition, we also analyse the turbulent kinetic energy budget, which is a quite good tool in attempt to further understand polymer–turbulence interactions. We believe that the comprehension of these interactions is the key to highlight the mechanism of DR.

2. PHYSICAL AND NUMERICAL METHODOLOGIES

A turbulent plane Couette flow of an incompressible dilute polymer solution is considered. Such a geometry represents one of the canonical ones and is commonly adopted in direct numerical simulations due its simplicity as well as its attractiveness for theoretical studies of near wall turbulent interactions.

Here, the plane Couette streamwise direction is $x_1 = x$, the spanwise direction is $x_2 = y$, and the wall-normal direction is $x_3 = z$. The flow is driven by both the top and the bottom plates, which have the same velocity magnitude in the streamwise direction (U_h) but opposite senses.

The instantaneous velocity field in the respective directions is $(u_x, u_y, u_z) = (u_1, u_2, u_3)$. In order to conduct comparative analysis of the inner layer dynamics of the plane Couette flow, wall scaling is used and based on zero-shear rate variables with the length and time scaled by ν_{tot}/u_τ and ν_{tot}/u_τ^2, where $\nu_{tot} = \nu_N + \nu_{p0}$ is the total (solvent + polymer) zero-shear viscosity, and u_τ is the zero-shear friction velocity. Using this scaling, the dimensionless conservation equations are

$$\frac{\partial u_j^+}{\partial x_j^+} = 0\,, \tag{1}$$

$$\frac{\partial u_i^+}{\partial t^+} + u_j^+ \frac{\partial u_i^+}{\partial x_j^+} = -\frac{\partial p^+}{\partial x_i^+} + \beta_0 \frac{\partial^2 u_i^+}{\partial {x_j^+}^2} + \frac{\partial \Xi_{ij}^+}{\partial x_j^+}\,. \tag{2}$$

In Eq. 2, the superscript '+' indicates the wall unit normalization, p^+ is the pressure, β_0 is the ratio of the Newtonian solvent viscosity (ν_N) to the total zero-shear viscosity (ν_{tot}). The extra-stress tensor components are denoted by Ξ_{ij}^+. The formalism of Eq. 2 includes the assumption of a uniform polymer concentration which is governed by the viscosity ratio β_0, where $\beta_0 = 1$ yields the limiting behaviour of the Newtonian case.

The extra-stress tensor components (Ξ_{ij}^+) in Eq. 2 represent the polymer's contribution to the tension of the solution. This contribution is accounted for by a single spring-dumbbell model. We employ here the FENE-P kinetic theory (Bird *et al.*, 1987), which is the most preferred one due to its physically realistic finite extensibility of the polymer molecules and to its relatively simple second-order closure. This model employs the phase-averaged conformation tensor $C_{ij} = \langle q_i q_j \rangle$, where the q_i are the components of the *end-to-end vector* of each individual polymer molecule. The extra-stress tensor is then

$$\Xi_{ij}^+ = \alpha_0 \left(f\left\{tr\left(\boldsymbol{C}\right)\right\} C_{ij} - \delta_{ij} \right)\,, \tag{3}$$

where $\alpha_0 = (1-\beta_0)/We_{\tau 0}$, $We_{\tau 0} = \lambda u_\tau^2/\nu_{tot}$ is the friction Weissenberg number representing the ratio of the elastic relaxation time (λ) relative to the viscous time scale. Additionally, δ_{ij} is the Kronecker delta operator and $f\left\{tr\left(\boldsymbol{C}\right)\right\}$ is given by the Peterlin approximation

$$f\left\{tr\left(\boldsymbol{C}\right)\right\} = \frac{L^2 - 3}{L^2 - tr\left(\boldsymbol{C}\right)}\,, \tag{4}$$

where L is the maximum polymer molecule extensibility and $\{tr\left(.\right)\}$ represents the trace operator. The equation system is closed with an evolution equation for the conformation tensor

$$\frac{DC_{ij}}{Dt} = \left(C_{ik}S_{kj}^+ + S_{ik}^+ C_{kj}\right) - \left(C_{ik}W_{kj}^+ + W_{ik}^+ C_{kj}\right) - \frac{f\left(tr\left(\boldsymbol{C}\right)\right) C_{ij} - \delta_{ij}}{We_{\tau 0}}\,, \tag{5}$$

where $S_{ij}^+ = \left(\partial u_i^+/\partial x_j^+ + \partial u_j^+/\partial x_i^+\right)/2$ and $W_{ij}^+ = \left(\partial u_i^+/\partial x_j^+ - \partial u_j^+/\partial x_i^+\right)/2$ are, respectively, the terms of the rate-of-strain, $\boldsymbol{S}^+$, and the rate-of-rotation, $\boldsymbol{W}^+$, tensors.

Since the numerical scheme for our direct numerical simulations (DNS) was already given in detail by Thais *et al.* (2011), we present here a brief description of the mathematical and numerical approaches. The hybrid MPI/OPENMP algorithm used was tailored to run properly in massively parallel architectures. The hybrid spatial scheme includes Fourier spectral accuracy in the two homogeneous directions (x and y) and sixth-order compact finite differences for the first and second-order wall-normal derivatives (z direction). Time marching can be up to fourth-order accurate by the use of the Adams–Moulton scheme for the viscous terms and Adams–Bashforth for the explicit terms. Pressure–velocity coupling is facilitated by a higher order generalization of the semi-implicit fractional step method on a non-staggered grid arrangement analysed by Armfield and Street (2000). In order to attenuate high wave-number energy accumulation, de-aliasing and fourth-order filtering are performed in the two homogeneous and wall-normal directions, respectively. Typically, this algorithm makes possible high-resolution, high drag reduction viscoelastic DNS, at relatively high flow Reynolds numbers.

In order to analyse the interaction of the polymer molecules with the turbulence from the very beginning to the steady state, the initial conditions for the conformation tensor was the identity tensor, $\boldsymbol{I}$ ($\boldsymbol{C} = \boldsymbol{I}$ at the beginning of the simulations). In addition, for each viscoelastic case, both the velocity and the pressure fields were initially started from the

same Newtonian fully developed turbulent flow. As a result of this methodology, DR exhibits a hight transient behaviour before achieving its statistical steady state, as we will show in the next section.

The parameters for the turbulent FENE-P plane Couette flows studied here are summarized in Table 1. We simulated our viscoelastic cases fixing the Reynolds number based on the plate velocities, $Re_h = hU_h/\nu_{tot}$, at 3000 and β at 0.9. Three combinations of Weissenberg number, $We_h = \lambda U_h/h$, and L were explored: $We_h = 10$ and $L = 100$; $We_h = 4.3$ and $L = 100$; $We_h = 10$ and $L = 30$. Both the size of the domain ($L_x \times L_y \times L_z = 12\pi \times 4\pi \times 2$) and the number of mesh points ($N_x \times N_y \times N_z = 384 \times 256 \times 129$) were kept the same for all cases, which leads in a grid resolution of $11.69 \leqslant \Delta x^+ \leqslant 13.40$, $5.85 \leqslant \Delta y^+ \leqslant 6.70$, and $0.31 \leqslant \Delta z^+ \leqslant 4.36$.

Table 1: Parameters for the turbulent FENE-P plane Couette flows. In this paper, three FENE-P flows were examined keeping $Re_h = 3000$ and $\beta = 0.9$ fixed. In addition, both the size of the domain ($L_x \times L_y \times L_z = 12\pi \times 4\pi \times 2$) and the number of mesh points ($N_x \times N_y \times N_z = 384 \times 256 \times 129$) were kept the same for all cases.

Re_h	$Re_{\tau 0}$	We_h	$We_{\tau 0}$	L	u_τ	Δ_x^+ **x** Δ_y^+ **x** $\Delta_{z,min}^+$	$\Delta_{z,max}^+$	**DR [%]**
3000	119.1	10	47.3	100	0.040	11.69 x 5.85 x 0.31	3.81	47
3000	136.5	4.3	26.7	100	0.046	13.40 x 6.70 x 0.35	4.36	30
3000	136.5	10	62.1	30	0.046	13.40 x 6.70 x 0.35	4.36	30

For the present study, we define the percentage of DR in time as follows:

$$DR(t) = \left(1 - \frac{\tau_w(t)}{\tau_w(t=0)}\right) \times 100\,, \tag{6}$$

where $\tau_w(t)$ is the wall shear stress at a given instant t and $\tau_w(t=0)$ is the wall shear stress at the very beginning of the simulation when polymers are totally coiled.

3. RESULTS AND DISCUSSION

The evolution of the vortical structures over time can be recognized in Fig. 1 in which three-dimensional isosurfaces of Q is displaced. The use of such a kind of entity to identify turbulent structures is quite common and is known as *Q-criterion*, in which vortical (or elliptical) structures are defined as the positive values of the second invariant of the velocity gradient tensor, computed for incompressible flows by:

$$Q = \frac{1}{2}\left(||\boldsymbol{W}||^2 - ||\boldsymbol{S}||^2\right) > 0\,, \tag{7}$$

where $||\boldsymbol{W}||$ and $||\boldsymbol{S}||$ denote the Euclidean norms of $\boldsymbol{W}$ and $\boldsymbol{S}$, respectively[1]. On the other hand negative values of Q indicate extensional (or hyperbolic) regions. For more details about such a criterion see Hunt *et al.* (1988). The structures shown in Fig. 1 come from the simulation of our most elastic FENE-P fluid ($We_h = 10$ and $L = 100$). From the top to the bottom, it is displaced four instantaneous three-dimensional structures of Q. Exceptionally in Fig. 1(*a*), we fixed $Q = 1$. At the very beginning of the simulation, $tU_h/h = 0.3$, the flow is full of structures and the isosurfaces of $Q = 0.1$ completely fill the domain. The colours on the isosurfaces depict the level of the relative polymer stretching, measured by the trace of the conformation tensor (normalized by the maximum polymer extension length), $tr\left(\boldsymbol{C}\right)/L^2$. At the very first instants of the simulation, the molecules are totally coiled, $tr\left(\boldsymbol{C}\right)/L^2 \approx 0$ (the blue colour is dominant). Without any interaction between polymers and turbulent structures, we see an apparently Newtonian fluid flow and the drag reduction is unmeasurable or practically null ($DR \approx 0\%$), which is expected.

Few instants later, at $tU_h/h = 9$, Fig. 1(*b*), the Newtonian morphology is completely changed. The polymers are abruptly stretched and the turbulent structures are partially destroyed (the vortices with $Q = 1$ completely vanished). The isosurfaces of $Q = 0.1$ do not completely fill the domain anymore, even though the number of structures is widely spread over it. The surfaces are quite coloured from blue ($tr(\mathbf{C})/L^2 \approx 0$) to red ($tr(\mathbf{C})/L^2 \approx 0.8$), which indicates a polymeric deformation distribution over the domain. It is not too easy to see from Fig. 1, but the stretching is higher close to the wall, where the mean shear stress is more intense (we will go back in this point later). We would like to emphasize right here that at $tU_h/h = 9$ the drag reduction is very negative ($DR \approx -60\%$), despite the disappearance of a great number of turbulent structures. Numerical simulations of FENE-P fluid which show drag increase were also reported by Dimitropoulos *et al.* (2005) and Tamano *et al.* (2011), who argue that polymers take the great part of the necessary energy for stretching from the mean shear flow and such a significant loss of energy is the main cause of an initial drag increase, even restraining part of the vortices. The same explanation was used by Andrade *et al.* (2014) who performed a number of experiments to take into account the drag increase and its dependence with polymer concentration and molecular weight.

In the sequence of the simulation, at $tU_h/h = 100$, Fig. 1(*c*), the turbulent structures with $Q = 0.1$ is strongly suppressed and the flow experiences its maximum level of drag reduction ($DR \approx 60\%$). The morphology of the vortices is very different from the Newtonian case, that at the beginning of the simulation, displayed in Fig. 1(*a*). Their thicknesses and streamwise lengths increase, while they become more parallel to the wall. After the maximum DR is reached, a

[1]The Euclidean norm of a generic second order tensor $\boldsymbol{A}$ is $||\boldsymbol{A}|| = \sqrt{tr\left(\boldsymbol{A}\cdot\boldsymbol{A}^{\boldsymbol{T}}\right)}$.

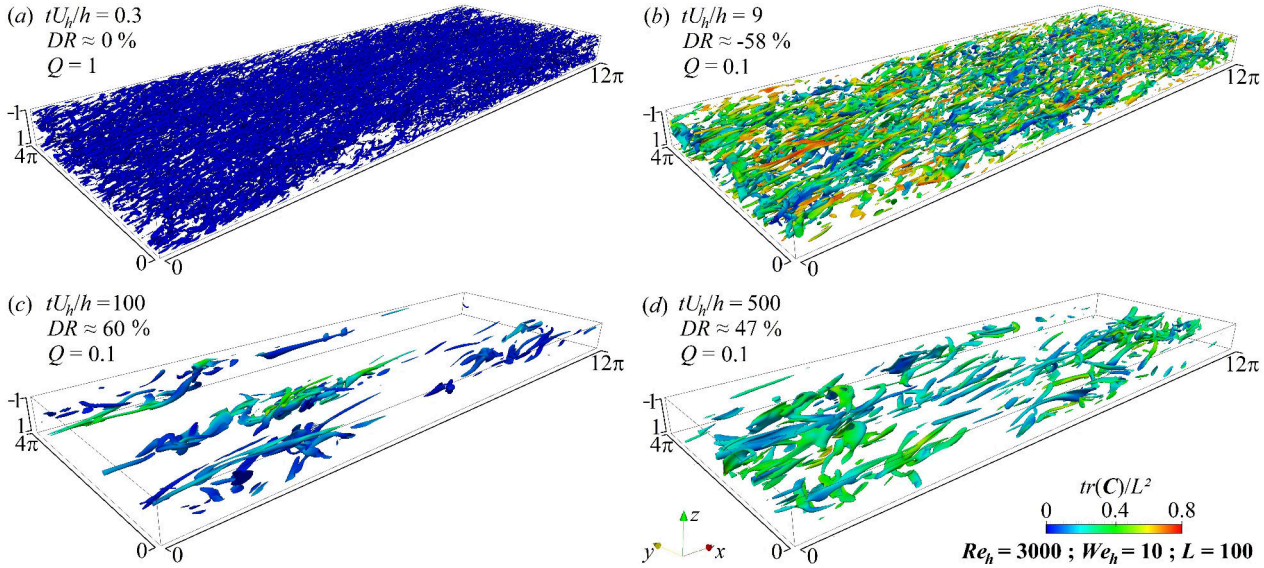

Figure 1: The three-dimensional structures represent isosurfaces of vortical regions defined as a positive value of the second invariant of velocity gradient tensor, $\nabla \boldsymbol{u}$. The colours indicate the polymer stretching, $tr\left(\boldsymbol{C}\right)/L^2$.

significant amount of structures appears again before finding its statistical steady state at $tU_h/h > 300$. In Fig. 1(*d*) we see the isosurfaces at $tU_h/h = 500$, in which the final value of DR is around 47%.

The initial interactions between polymers and turbulent structures impose a transient behaviour on the drag reduction level at the very beginning of the phenomenon, as highlighted in Fig. 2(*b*) for our three viscoelastic cases. The drag reduction level is compared with the spatial average of the relative polymer stretching, $< tr\left(\boldsymbol{C}\right)/L^2 >_{xyz}$, presented in Fig. 2(*a*), revealing an asynchronism between these two quantities. The asynchronous behaviour is obvious. At the very beginning, there is not interaction between polymers and turbulent structures and, consequently, DR and $< tr\left(\boldsymbol{C}\right)/L^2 >_{xyz}$ are zero. A few instants after, the molecules start to be stretched, mainly by the mean shear flow (in fact, polymers also take a non-negligible amount of energy from the turbulent structures), and $< tr\left(\boldsymbol{C}\right)/L^2 >_{xyz}$ increases until reaching its maximum value (such a maximum value occurs at $tU_h/h = 9$ for the most viscoelastic FENE-P fluid). Simultaneously, DR significantly falls and its maximum negative value of -60% is reached, which indicates an expressive drag increase. Thus, the minimum DR (or the maximum drag increase) occurs when the molecules have their maximum mean length, which is a diametrical asynchronism. As we mentioned before, it occurs because the polymers take energy for stretching primarily from the mean shear flow and the consequence is the decrease of DR. As the elastic parameters are incremented, the drag increase becomes more evident ($DR \approx -20\%$ for $We_h = 10$ and $L = 30$, and $DR \approx -60\%$, for $We_h = 10$ and $L = 100$). This is in accordance with the experiments available in Andrade *et al.* (2014). The increase of polymer concentration or molecular weight in a solution induces an increase on the drag at the very start of the drag reducing flow. The authors argue that the necessary energy used to change the polymers from their coiled state to a stretched new configuration increases when a greater amount of molecules is introduced in the solvent. The same happens if the molecular weight is increased. A larger molecule store more energy when stretched. Now concerning our simulations, if we increase polymer concentration and molecular weight, the Weissenberg number also increases, since the relaxation time is an increasing function of concentration. Hence, we see that our current numerical data are in a good qualitative agreement with the experiments reported in Andrade *et al.* (2014).

After its minimum value, DR starts to increase and simultaneously $< tr\left(\boldsymbol{C}\right)/L^2 >_{xyz}$ decreases until the maximum value of drag reduction is reached. Such a maximum occurs at the dimensionless time equal to 100 for the most viscoelastic FENE-P fluid (grey circles). Some instants after the phenomenon achieve its steady state regime, from an average point of view. As pointed before, the maximum and the minimum values of DR is an increasing function of L and We_h, which is in fully accordance with the experiments in Andrade *et al.* (2014). Hence, the polymer stretching and the drag reduction do not follow the same rate. In fact, they are totally asynchronous. Such a behaviour was also observed by Dimitropoulos *et al.* (2005), analysing a turbulent flow of FENE-P fluid in a different geometry. Hence, as we argued in Andrade *et al.* (2014), the turbulent flow is disturbed by the polymers at the very few instants of the process. There is a change of energy between the mean flow, vortices and polymers and such an interaction induces a strong transient behaviour, which reaches its statistical steady state after a period of time, called here developing time, t_d. This time is also a strong increasing function of the elasticity (L and We_h). Again, this is in accordance with the experiments in Andrade *et al.* (2014), where it is observed an increasing t_d with polymer concentration and molecular weight.

It is worth noting in Figure 2(*a*) how L and We_h affect the polymeric deformation. Hence, let us compare the grey circles ($We_h = 10$; $L = 100$) and the red diamonds ($We_h = 10$; $L = 30$). It can be clearly seen that the relative polymer extension decreases with increasing L, which suggests that larger polymer molecules are less susceptible to chain scission, as pointed out by Pereira and Soares (2012). In opposing trend, $tr(\boldsymbol{C})/L^2$ increases with We_h. If the relaxation time increases, polymers can interact with a more extensive spectrum of turbulent structures (see also Dallas *et al.*, 2010).

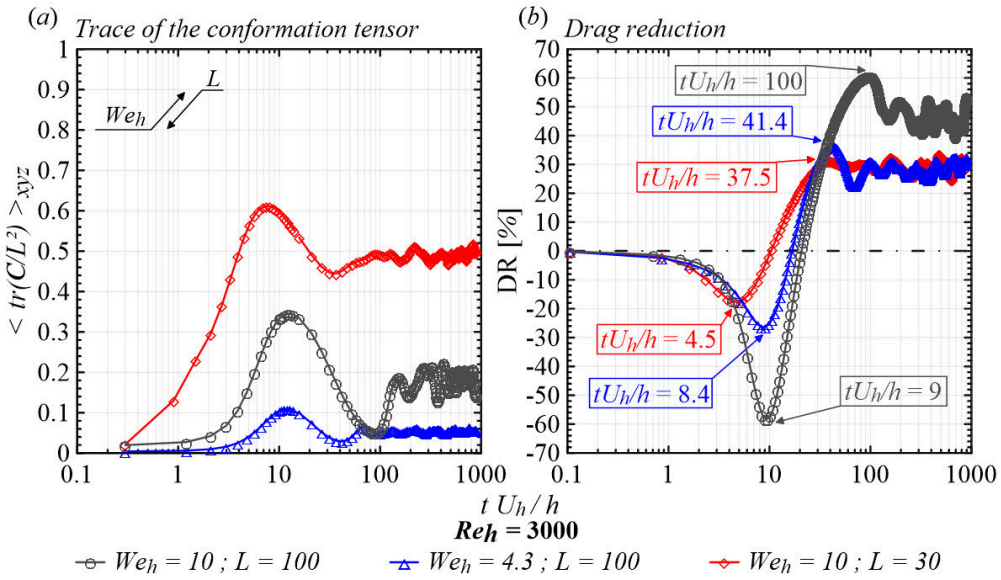

Figure 2: Evolution of the spatial average of the relative polymer stretching as function of the normalized time, tU_h/h (a). Average drag reduction, DR, as function of the normalized time (b).

Thus, their stretching must be more pronounced. This is also in agreement with Pereira and Soares (2012).

In order to better understand the interactions between the turbulence and the polymer, we displayed respectively in Figs. 3(a) and (b) the average values in the $x-y$ plane of the trace of the normalized conformation tensor, $\langle tr\left(\boldsymbol{C}\right)/L^2\rangle$, and the streamwise velocity component for the most elastic case. In order to compare our profiles with the classical ones available in literature, the velocity of the bottom plate was subtracted from the velocity field, resulting in a relative streamwise component u_{rx} given by $u_{rx} = u_x - (-U_h)$. We choose some very specific instants for each viscoelastic case, as those for the maximum drag increase and drag reduction (values of tU_h/h inside the boxes in Fig. 2b), in addition to an instant at the very beginning of the simulation and at that correspondent to the statistical steady state.

Concerning the Fig. 3(a), polymers are considerably stretched near the wall, within the *viscous sublayer* ($0 < z+ < 5$; region I), where the mean turbulent shear flow are very intense. The maximum deformation occurs in the Newtonian *buffer layer* ($5 < z+ < 30$; region II) and it dramatically decreases in the Newtonian *log-law region* ($z^+ > 30$; region III). Obviously, at the very start of the simulation, $tU_h/h = 0.3$, the mean polymer stretching is zero (grey circles). It reaches its maximum value some instants after (blue triangles), before decrease again until finding a new minimum (red diamonds). At dimensionless times 500 and 1000, the polymer deformation is in its statistical steady state.

Analysing the Fig. 3(b), we observe that, close to the wall (region I) all velocity profiles fall dawn in the *viscous law* ($< u^+_{rx} >= z^+$; solid grey line), as expected. At the very start of the simulation, $tU_h/h = 0.3$, the polymers were totally coiled and the velocity profile fitted the Newtonian *log-law* (grey dots). Hence, at the beginning of the simulation the FENE-P behaves as a Newtonian fluid, because the molecules are not significantly stretched. Some instants after, when the maximum drag increase is reached, the velocity profile is below the Newtonian (blue triangles). This is quite representative and a clear picture of what happens to the mean flow, which is retarded when polymers take energy from it to be stretched. Such retardation is really impressive for the most viscoelastic FENE-P fluid. The velocity profile for the maximum drag reduction conduction is in red diamonds. It is worth noting that the MDR asymptote (red dash-dotted line) is achieved at $tU_h/h = 100$, when the maximum DR is reached (see Fig. 2b), before getting down to find its steady state (green squares and orange inverted triangles).

The results discussed above indicate an expressive interaction between the polymer and the flow during the beginning of the drag reduction phenomenon followed by a significant energy exchanges. Aiming to characterize such energy exchanges, we consider the work equation

$$\underbrace{\left[\frac{1}{2}\frac{\partial\left(u_\alpha^{+2}\right)}{\partial t^+}\right]}_{T_\alpha^+} = \underbrace{\left[-u_\alpha^+\frac{\partial\left(u_\alpha^+u_i^+\right)}{\partial x_i^+}\right]}_{A_\alpha^+} + \underbrace{\left[-u_\alpha^+\frac{\partial p^+}{\partial x_\alpha^+}\right]}_{P_\alpha^+} + \underbrace{\left[\left(\beta_0\right)u_\alpha^+\frac{\partial^2 u_\alpha^+}{\partial x_i^{+2}}\right]}_{V_\alpha^+} + \underbrace{\left[u_\alpha^+\frac{\partial \Xi_{\alpha i}^+}{\partial x_i^+}\right]}_{E_\alpha^+}, \tag{8}$$

where the instantaneous polymer work term, E_α^+, indicates the amount of energy stored ($E_\alpha^+ < 0$) or released ($E_\alpha^+ > 0$) by polymers from the velocity field in the α direction, u_α^+. The complementary work terms denote the advection A_α^+, the pressure redistribution P_α^+, and the viscous stress V_α^+. The sum $A_\alpha^+ + P_\alpha^+ + V_\alpha^+$ is referred as *Newtonian work*, N_α^+, and T_α^+ is the time derivative energy term.

The kinetic energy terms presented above are displayed in Fig. 4 as a function of the normalized wall distance. The analysis is restricted to the most viscoelastic FENE-P fluid. Again we see that, at the very beginning, $tU_h/h = 0.3$, the polymeric work (blue crosses) is zero and the kinetic energy is balanced by the Newtonian terms (orange inverted

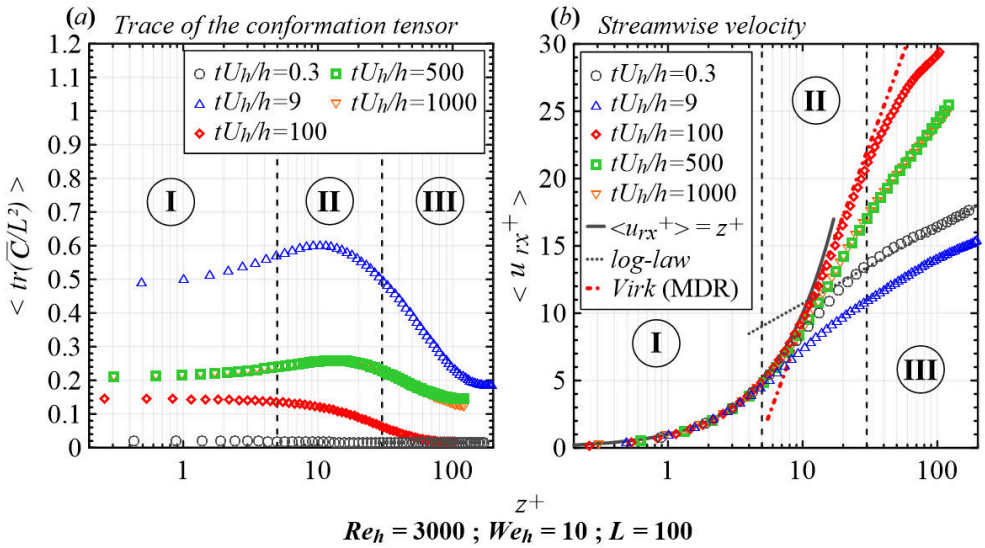

Figure 3: Average values in the $x-y$ plane of the trace of the normalized conformation tensor, $\langle tr\left(\boldsymbol{C}\right)/L^2\rangle$, as function of the normalized wall distance for the most viscoelastic flow (*a*). Average values in the $x-y$ plane of the streamwise relative velocity, $\langle u_{rx}^{+}\rangle$, as function of the normalized wall distance for the most viscoelastic flow (*b*).

triangles). More precisely, the advection term $< A_x^+ >$ balances the viscous dissipation $< V_x^+ >$. Both quantities are nulls at the wall and reach their maximum values in the buffer, just above the viscous sublayer ($z^+ \approx 5.5$). It seems that $< A_x^+ >$ and $< V_x^+ >$ are the main terms in flow of Newtonian fluids, the former being the most important one as pointed by Graham (2015). At the logarithmic zone, region III, both the terms significantly reduce. Such a behaviour is expected, since the viscous dissipations in flows of Newtonian fluids are related to the small scale fluctuations, which are nulls very close to walls and less significant in the core region. After $tU_h/h = 9$, the energy distribution dramatically changes (Fig. 4*b*). The polymeric work starts to play a very important role in the flow. At this time, when the maximum drag increase occurs, the energy is exclusively balanced by the polymeric work and the viscous dissipation, since $< A_x^+ >$ is strongly suppressed across the plane Couette half-width and $< P_x^+ >$ plays a minor role. As discussed previously, polymers are primarily stretched by the mean shear flow close to the wall, which implies an intense polymeric work in the viscous sublayer, region I. In addition, turbulent structures interact with the molecules, providing a supplementary polymer extension over the geometry. In other words, the mean shear flow is responsible for a relevant polymer pre-stretching, which is incremented since the turbulent structures interact with the polymer molecules, providing a supplementary polymer extension. After the accentuated polymer deformation at the beginning of the simulation, the molecules reduce their mean length and release energy to the mean flow. A significant increment on the advection term $< A_x^+ >$ is then perceived in Fig. 4(*c*), which results from the fact that the mean flow also act as a source of turbulent energy, as mentioned before. At this time, $tU_h/h = 100$, we observe the maximum drag reduction ($DR \approx 60\%$). Lastly, the energy in the statistical steady state condition, Fig. 4(*d*), is balanced by the polymeric work, the viscous dissipation, and the advection terms. In fact, comparing Figs. 4(*a*) and (*d*), we observe that $< A_x^+ >$ is strongly suppressed by the polymers within the buffer layer, a consequence of the weakening of the turbulent structures evidenced in Fig. 1.

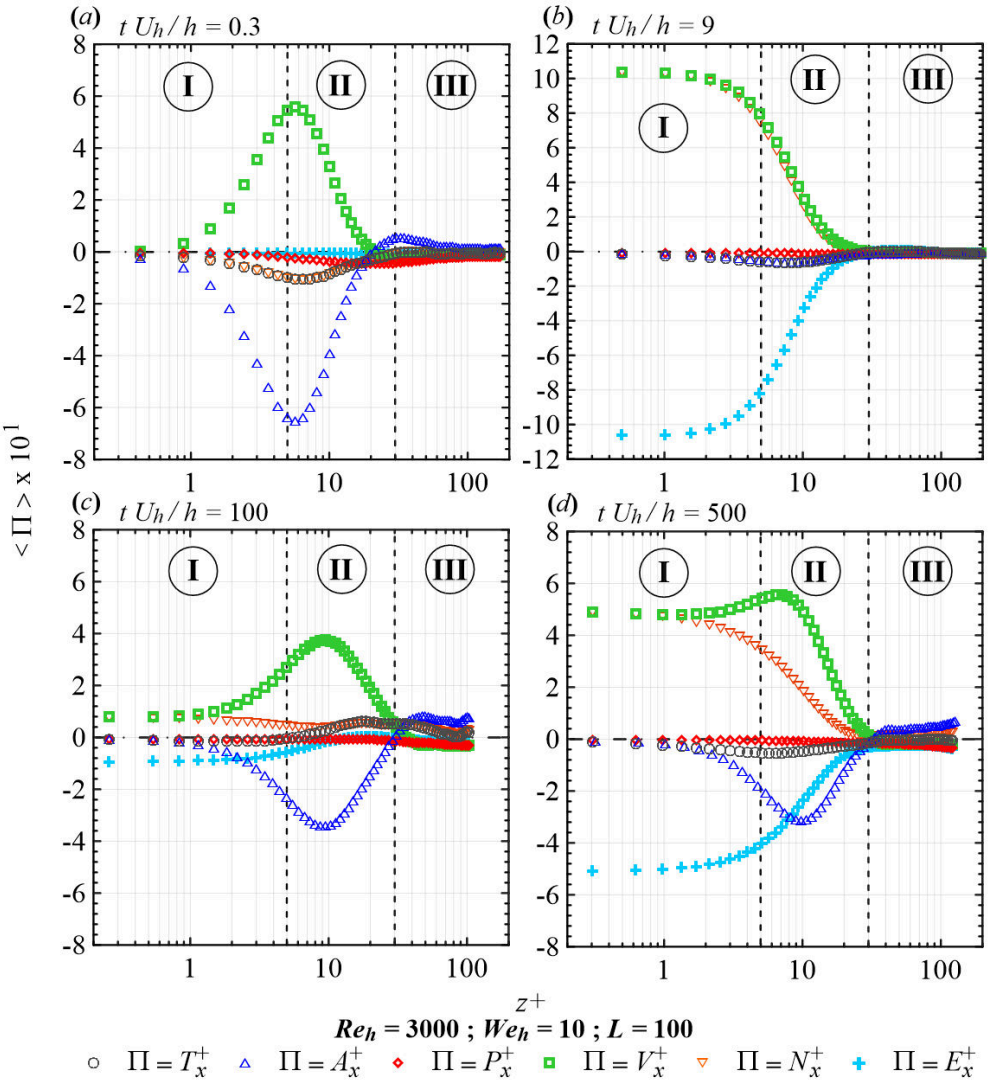

Figure 4: Average values in the $x-y$ plane of the streamwise turbulent kinetic energy budget against the normalized wall distance.

4. CONCLUDING REMARKS

We use here direct numerical simulations of FENE-P fluid to analyse a time–dependent drag reducing flow between parallel plates fixing the Reynolds number and viscosity ratio. We simulated three viscoelastic cases changing the values of We_h and L. Our main interest was to pick out and emphasize some transient features of the drag reducing flow throughout parallel plates in attempt to further understand its mean mechanism. The analyses of the simulations clearly show that three entities play a very important role on $DR(t)$, namely here: mean shear flow, polymeric stretching and turbulent structures. Energy is constantly exchanged between those quantities from the beginning of the simulation until its statistical steady state and it is the key to understand drag reduction in function of time.

The drag reduction level assumes a significant negative value at the beginning of the simulation because polymers take an expressive amount of energy from the mean flow in order to initially stretch. Consequently, during this period, the velocity profiles are below the Newtonian, which indicates an increase of the drag.

Another point which import to remark is that the asymptotic drag reduction is below its maximum value. This is not obvious, but can be explained by means of fluid dynamics. In fact, DR and the polymer stretching oscillates until finding a statistical steady state after a long time due to the strong exchanges of energy, which dramatically changes the flow over time as well as DR and the polymer conformation.

5. ACKNOWLEDGEMENTS

This research was granted access to the HPC resources of IDRIS under the allocation 2014-i20142b2277 made by GENCI. The authors are also grateful for the Brazilian Scholarship Program supported by Brazilian Research Council (CNPq).

Andrade, R.M., Pereira, A.S. and Soares, E.J., 2014. "Drag increase at the very start of drag reducing flows in a rotating cylindrical double gap device". *Journal of Non-Newtonian Fluid Mechanics*, Vol. 212, pp. 73–79.

Andrade, R.M., Pereira, A.S. and Soares, E.J., 2016. "Drag reduction in synthetic seawater by flexible and rigid polymer addition into a rotating cylindrical double gap device". *Journal of Fluids Engineering*, Vol. 138, pp. 021101–1–021101–10.

Armfield, S.W. and Street, R.L., 2000. "Fractional step methods for the navier–stokes equations on non-staggered grids". *ANZIAM J*, Vol. 42(E), pp. C134–C156.

Bird, R., Armstrong, R. and Hassager, O., 1987. *Dynamics of Polymeric Liquids. Kinetic Theory*. Wiley-Interscience.

Burger, E.D. and Chorn, L.G., 1980. "Studies of drag reduction conducted over a broad range of pipeline conditions when flowing Prudhoe Bay crude oil". *J. Rheology*, Vol. 24, p. 603.

Dallas, V., Vassilicos, J.C. and Hewitt, G.F., 2010. "Strong polymer–turbulence interactions in viscoelastic turbulent channel flow". *Physical Review E*, Vol. 82, pp. 066303–1–066303–19.

Dimitropoulos, C.D., Dubief, Y., Shaqfeh, E.S.G., Moin, P. and Lele, S.K., 2005. "Direct numerical simulation of polymer-induced drag reduction in turbulent boundary layer flow". *Physics of Fluids*, Vol. 17, pp. 1–4.

Fabula, A.G., 1971. "Fire-fighting benefits of polymeric friction reduction". *Trans ASME J Basic Engng*, pp. 93–453.

Forrest, F. and Grierson, G.A., 1931. "Friction losses in cast iron pipe carrying paper stock". *Paper Trade Journal*, Vol. 92, pp. 39–41.

Golda, J., 1986. "Hydraulic transport of coal in pipes with drag reducing additives". *Chem Engng Commun*, Vol. 45, pp. 53–67.

Graham, M.D., 2015. "Turbulence spreads like wildfire". *Nature*, Vol. 526, pp. 508–509.

Hunt, J.C.R., Wray, A.A. and Moin, P., 1988. "Eddies, stream, and convergence zones in turbulent flows". *Center for Turbulence Research - Proceedings of Summer Program*, Vol. Report CTR-S88, pp. 193–208.

Lumley, J.L., 1969. "Drag reduction by additives". *Annual Review of Fluid Mechanics*, Vol. 11, pp. 367–384.

Lumley, J.L., 1973. "Drag reduction in turbulent flow by polymer additives". *Journal of Polymer Science: Macromolecular Reviews*, Vol. 7, pp. 263–290.

Mysels, K.J., 1949. "Flow of thickened fluids". *U.S. Patent*, Vol. 2 Dec. 27 492, p. 173.

Pereira, A.S., Andrade, R.M. and Soares, E.J., 2013. "Drag reduction induced by flexible and rigid molecules in a turbulent flow into a rotating cylindrical double gap device: Comparison between poly (ethylene oxide), polyacrylamide, and xanthan gum". *Journal of Non-Newtonian Fluid Mechanics*, Vol. 202, pp. 72–87.

Pereira, A.S. and Soares, E.J., 2012. "Polymer degradation of dilute solutions in turbulent drag reducing flows in a cylindrical double gap rheometer device". *Journal of Non-Newtonian Fluid Mechanics*, Vol. 179, pp. 9–22.

Sellin, R.H.J., Hoyt, J.W., Poliert, J. and Scrivener, O., 1982. "The effect of drag reducing additives on fluid flows and their industrial applications Part ii: Present applications and future proposals". *Journal of Hydraulic Research*, Vol. 20, pp. 235–292.

Tabor, M. and de Gennes, P.G., 1986. "A cascade theory of drag reduction". *Europhysics Letter*, Vol. 2, pp. 519–522.

Tamano, S., Graham, M.D. and Morinishi, Y., 2011. "Streamwise variation of turbulent dynamics in boundary layer flow of drag-reducing fluid". *Journal of Fluid Mechanics*, Vol. 686, pp. 352–377.

Thais, L., Tejada-Martinez, A., Gatski, T.B. and Mompean, G., 2011. "A massively parallel hybrid scheme for direct numerical simulation of turbulent viscoelastic channel flow". *Computers and Fluids*, Vol. 43, pp. 134–142.

Toms, B.A., 1948. "Some observations on the flow of linear polymer solutions through straight tubes at large reynolds numbers". *Proceedings of the International Congress of Rheology, Holland, North-Holland, Amsterdam, Section II*, pp. 135–141.

Virk, P.S., 1975. "Drag reduction fundamentals". *AIChE Journal*, Vol. 21, pp. 625–656.

White, C.M. and Mungal, M.G., 2008. "Mechanics and prediction of turbulent drag reduction whit polymer additives". *Annual Review of Fluid Mechanics*, Vol. 40, pp. 235–256.

6. RESPONSIBILITY NOTICE

The following text, properly adapted to the number of authors, must be included in the last section of the paper: The author(s) is (are) the only responsible for the printed material included in this paper.